

# BER Analysis of Space Shift Keying in Cooperative Multi-hop Multi-branch DF Relaying

Pritam Som and A. Chockalingam

Department of ECE, Indian Institute of Science, Bangalore 560012

**Abstract**—Space shift keying (SSK) is an attractive modulation technique for multi-antenna communications. In SSK, only one among the available transmit antennas is activated during one channel use, and the index of the chosen transmit antenna conveys information. In this paper, we analyze the performance of SSK in *multi-hop, multi-branch* cooperative relaying systems. We consider the decode-and-forward relaying protocol, where a relay forwards the decoded symbol if it decodes the symbol correctly from the received signal. We derive closed-form expressions for the end-to-end bit error rate of SSK in this system. Analytical and simulation results match very well.

**Keywords** — Space shift keying, decode-and-forward, multi-hop, multi-branch, BER analysis.

## I. INTRODUCTION

Spatial modulation (SM) is a relatively new modulation technique for multi-antenna communication systems [1]. In this modulation technique, only one among the available transmit antennas is activated during signal transmission, and information is conveyed by the index of the active antenna. This helps in addressing the issues related to multiple antenna transmission, e.g., 1) inter-antenna synchronization, and 2) complexity, size and cost of hardware due to the use of multiple transmit radio frequency chains. Space shift keying (SSK) is a special case of SM [2], where a signal known to the receiver (say +1) is transmitted from the active transmit antenna. In a  $n_s = 2^m$  transmit antenna system, each antenna is mapped to a distinct information bit sequence of length  $m$ . This transmitting antenna, at any instant, is chosen based on the  $m$  information bits at that instant. At the receiver, the detection involves the determination of the index of the active transmit antenna based on the received signal. Thus, the information bit sequence associated with the detected transmit antenna index is conveyed to the receiver.

Recent works [3]-[8] have considered the concept of SM/SSK in relay assisted communication. SM was considered for decode-and-forward (DF) non-cooperative dual-hop relay channel in [3]. In [4], [5], a modulation scheme based on SSK, namely space time shift keying, has been proposed for cooperative communication. An information guided relaying scheme based on the concept of SSK was studied in [6]. In [7], the bit error rate (BER) performance of SSK in amplify-and-forward (AF) dual-hop relay channel in the absence of direct link between the source and the destination was analyzed. In [8], the BER analysis of dual-hop cooperative net-

work with multiple relays for DF and AF relaying protocol was presented.

The performance of general multi-branch multi-hop cooperative network has been studied for conventional QAM/PSK modulation in [9]-[13]. The performance of AF multi-hop multi-branch cooperative relay network has been analyzed for variable gain relays in [9], for fixed gain relays in [10], for channel state information assisted cooperative network in [11], and for log-normal fading in [12]. The performance in the presence of co-channel interference has been analyzed in [13]. In this paper, we consider *SSK modulation in multi-hop multi-branch cooperative network* and analyze its BER performance. We consider DF relaying, where, in a given hop, only those relays which decode the SSK symbol correctly forward the decoded symbol to the next hop. We derive closed-form expressions for the end-to-end BER, and validate the analytical results through simulation.

The rest of the paper is organized as follows. The system model is presented in Section II. The BER analysis is presented in Section III. Analytical and simulation results on the BER performance are presented in Section IV. Conclusions are presented in Section V.

## II. SYSTEM MODEL

We consider a general multi-hop multi-branch cooperative network consisting of source node S, destination node D, and  $L + 1$  diversity branches  $B_0, B_1, \dots, B_L$ , connecting S and D. The branch  $B_0$  denotes the direct S-to-D link. The branches  $B_1, \dots, B_L$  contain  $M_1, \dots, M_L$  relay nodes, respectively, as shown in Figure 1. The  $k$ th relay in the branch  $B_l$  is denoted as  $R_{k,l}$ . The source and relays are each equipped with  $n_s$  transmit antennas. The SSK symbol alphabet is given by

$$\begin{aligned} \mathbb{S}_{n_s} &\equiv \{\mathbf{s}_j : j = 1, \dots, n_s\}, \\ \mathbf{s}_j &= [0, \dots, 0, \underbrace{1}_{j\text{th coordinate}}, 0, \dots, 0]^T. \end{aligned} \quad (1)$$

The relay  $R_{k,l}$  and the destination D are equipped  $n_{rk,l}$  and  $n_d$  receive antennas, respectively. In the first phase, S broadcasts the SSK signal  $\mathbf{x}$ , which is heard by D and all the relays in the first hop of the branches  $B_1, \dots, B_L$ , i.e.,  $R_{1,1}, \dots, R_{1,L}$ , respectively. The received signal vectors at  $R_{1,l}$  and D, respectively, are given by

$$\mathbf{y}_{sr_1,l} = \mathbf{H}_{sr_1,l} \mathbf{x} + \mathbf{w}_{sr_1,l}, \quad l = 1, 2, \dots, L \quad (2)$$

$$\mathbf{y}_{sd} = \mathbf{H}_{sd} \mathbf{x} + \mathbf{w}_{sd}, \quad (3)$$

\* This work was supported in part by a gift from the Cisco University Research Program, a corporate advised fund of Silicon Valley Community Foundation.

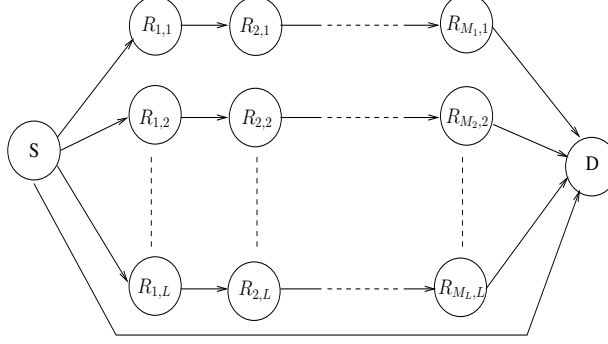


Fig. 1. System model of multi-hop multi-branch cooperative network.

where  $\mathbf{H}_{sr_1,l} \in \mathbb{C}^{n_{r_1,l} \times n_s}$  is the S-to- $R_{1,l}$  channel matrix,  $\mathbf{w}_{sr_1,l} \in \mathbb{C}^{n_{r_1,l} \times 1}$  is the additive noise vector at  $R_{1,l}$ ,  $\mathbf{H}_{sd} \in \mathbb{C}^{n_d \times n_s}$  is the S-to-D channel matrix, and  $\mathbf{w}_{sd} \in \mathbb{C}^{n_d \times 1}$  is the additive noise vector at D. We consider DF relaying. Each relay in the first hop of every branch ( $R_{1,l}; l = 1, 2, \dots, L$ ) decodes the signal in the first phase of communication and forwards to the next hop relays only if it decodes correctly. Likewise, at every hop, the relays in each diversity branch forward the regenerated symbol if the decoding is correct. This relaying protocol has been considered for SSK in dual-hop multiple relay cooperative system in [8]. Each branch  $B_l$ , that correctly decodes the signal at the relay terminal  $R_{M_l,l}$ , forwards the decoded SSK signal to D in different time slots. Let  $\mathbb{U}$  denote the set of the indices of the diversity branches that forward to the destination D. Without loss of generality, let us assume the case where the cardinality of  $\mathbb{U}$  denotes  $n$  ( $0 \leq n \leq L$ ).  $n = 0$  corresponds to the case when  $\mathbb{U}$  is null set, i.e., no multi-hop diversity branch can decode signal correctly. When  $n > 0$ , the elements of  $\mathbb{U}$  are denoted as  $u_1, u_2, \dots, u_n$ , respectively. Here,  $1 \leq u_1, \dots, u_n \leq L$ , and  $u_1 \neq u_2 \neq \dots \neq u_n$ . The destination combines the signal vectors and carries out optimal detection. The combined received vector is represented as

$$\begin{bmatrix} \mathbf{y}_{sd} \\ \mathbf{y}_{M_{u_1}d,u_1} \\ \vdots \\ \mathbf{y}_{M_{u_n}d,u_n} \end{bmatrix} = \begin{bmatrix} \mathbf{H}_{sd} \\ \mathbf{H}_{M_{u_1}d,u_1} \\ \vdots \\ \mathbf{H}_{M_{u_n}d,u_n} \end{bmatrix} \mathbf{x} + \begin{bmatrix} \mathbf{w}_{sd} \\ \mathbf{w}_{M_{u_1}d,u_1} \\ \vdots \\ \mathbf{w}_{M_{u_n}d,u_n} \end{bmatrix}, \quad (4)$$

where  $\mathbf{y}_{M_{u_1}d,u_1}, \dots, \mathbf{y}_{M_{u_n}d,u_n}$  are the received signal vectors from the relay nodes  $R_{M_{u_1},u_1}, \dots, R_{M_{u_n},u_n}$ , respectively.  $\mathbf{H}_{M_{u_1}d,u_1}, \dots, \mathbf{H}_{M_{u_n}d,u_n}$  are the  $R_{M_{u_1},u_1}$ -to-D,  $\dots$ ,  $R_{M_{u_n},u_n}$ -to-D channel matrices, respectively.  $\mathbf{w}_{M_{u_1}d,u_1}, \dots, \mathbf{w}_{M_{u_n}d,u_n}$  are the noise vectors at D. The detected signal at D is given by

$$\tilde{\mathbf{x}} = \min_{s \in \mathbb{S}_{n_s}} \|\mathbf{y} - \mathbf{H}s\|^2. \quad (5)$$

The elements of the noise vectors are modelled as i.i.d.  $\mathcal{CN}(0, \sigma^2)$ . The channel matrix between the nodes  $R_{k-1,l}$  and  $R_{k,l}$  at the branch  $B_l$  for  $k = 2, \dots, M_l$  is denoted as  $\mathbf{H}_{k-1,k,l}$ .

The entries of the channel matrices  $\mathbf{H}_{sd}$ ,  $\mathbf{H}_{sr_1,l}$ ,  $\mathbf{H}_{k-1,k,l}$ , and  $\mathbf{H}_{M_l d, l}$  are modelled as  $\mathcal{CN}(0, \sigma_{sd}^2)$ ,  $\mathcal{CN}(0, \sigma_{sr_1,l}^2)$ ,  $\mathcal{CN}(0, \sigma_{k-1,k,l}^2)$ , and  $\mathcal{CN}(0, \sigma_{M_l d, l}^2)$ , respectively, where  $\sigma_{sd}^2$ ,  $\sigma_{sr_1,l}^2$ ,  $\sigma_{k-1,k,l}^2$ , and  $\sigma_{M_l d, l}^2$  depend on the path loss and shadowing in the corresponding links. The channel matrices in each link are assumed to be independent of each other.

### III. BER ANALYSIS

#### A. Analysis for $n_s = 2$

We denote the end-to-end error event in detection of bits as  $E$ . Let  $\psi$  denote the set of indices of the diversity branches that decode the signal correctly and forward the decoded signal to destination. The end-to-end BER can be written as

$$P(E) = \sum_{\psi \in \mathcal{P}(\{1, 2, \dots, L\})} P(\psi) P(E|\psi), \quad (6)$$

where  $\mathcal{P}(\{1, 2, \dots, L\})$  is the power set of the set of the indices of the diversity branches  $\{1, 2, \dots, L\}$ . Without loss of generality, let us consider the case when  $\psi = \mathbb{U}$ , where  $\mathbb{U}$  is the set of indices of the diversity branches as defined in Section II. Then, from (4), the conditional probability of error  $P(E|\psi = \mathbb{U}; \mathbf{H}_{M_{u_i}d,u_i}, u_i \in \mathbb{U})$  can be written as [2]

$$\begin{aligned} P(E|\psi = \mathbb{U}; \mathbf{H}_{M_{u_i}d,u_i}, u_i \in \mathbb{U}) \\ = Q\left(\sqrt{\frac{\|\mathbf{h}^1 - \mathbf{h}^2\|^2}{2\sigma^2}}\right) \end{aligned} \quad (7)$$

$$= Q(\sqrt{\Lambda}). \quad (8)$$

Here,  $\mathbf{h}^q$  is the  $q$ th column of  $\mathbf{H}$  and  $\|\mathbf{h}^1 - \mathbf{h}^2\|^2 = \|\mathbf{h}_{sd}^1 - \mathbf{h}_{sd}^2\|^2 + \sum_{i=1}^n \|\mathbf{h}_{M_{u_i}d,u_i}^1 - \mathbf{h}_{M_{u_i}d,u_i}^2\|^2$ .  $\mathbf{h}_{sd}^q$ ,  $\mathbf{h}_{M_{u_i}d,u_i}^q$  are the  $q$ th columns of  $\mathbf{H}_{sd}$  and  $\mathbf{H}_{M_{u_i}d,u_i}$ , respectively.  $\Lambda$  is the sum of  $n+1$  independent Gamma distributed random variables and can be written as

$$\Lambda = \Lambda_{sd} + \sum_{i=1}^n \Lambda_{M_{u_i}d,u_i}^{u_i}, \quad (9)$$

where  $\Lambda_{sd} = \frac{\|\mathbf{h}_{sd}^1 - \mathbf{h}_{sd}^2\|^2}{2\sigma^2}$  and  $\Lambda_{M_{u_i}d,u_i}^{u_i} = \frac{\|\mathbf{h}_{M_{u_i}d,u_i}^1 - \mathbf{h}_{M_{u_i}d,u_i}^2\|^2}{2\sigma^2}$  are distributed as  $\Gamma_v(n_d, \Omega_{sd})$  and  $\Gamma_v(n_d, \Omega_{M_{u_i}d,u_i})$ , respectively, and  $\Omega_{sd} = \frac{\sigma_{sd}^2}{\sigma^2}$ ,  $\Omega_{M_{u_i}d,u_i} = \frac{\sigma_{M_{u_i}d,u_i}^2}{\sigma^2}$ . Here,  $\Gamma_v(a, b)$  denotes Gamma distribution of shape parameter  $a$  and scale parameter  $b$ .

Averaging (8), the conditional error probability  $P(E|\psi = \mathbb{U})$  can be written as

$$\begin{aligned} P(E|\psi = \mathbb{U}) \\ = \int_0^\infty Q(\sqrt{\lambda}) f_\Lambda(\lambda) d\lambda \\ = \int_0^\infty \frac{1}{\pi} \int_0^{\frac{\pi}{2}} \exp\left(-\frac{\lambda}{2\sin^2\theta}\right) d\theta f_\Lambda(\lambda) d\lambda \\ = \frac{1}{\pi} \int_0^{\frac{\pi}{2}} \int_0^\infty \exp\left(-\frac{\lambda}{2\sin^2\theta}\right) f_\Lambda(\lambda) d\lambda d\theta \\ = \frac{1}{\pi} \int_0^{\frac{\pi}{2}} G_\Lambda\left(-\frac{1}{2\sin^2\theta}\right) d\theta \end{aligned} \quad (10)$$

$$\begin{aligned}
&= \frac{1}{\pi} \int_0^{\frac{\pi}{2}} G_{\Lambda_{sd}}\left(-\frac{1}{2 \sin ^2 \theta}\right) \prod_{i=1}^n G_{\Lambda_{M_{u_i} d}^{u_i}}\left(-\frac{1}{2 \sin ^2 \theta}\right) d \theta \\
&=\frac{1}{\pi} \int_0^{\frac{\pi}{2}}\left(1+\frac{\Omega_{s d}}{2 \sin ^2 \theta}\right)^{-n_d} \prod_{i=1}^n\left(1+\frac{\Omega_{M_{u_i} d, u_i}}{2 \sin ^2 \theta}\right)^{-n_d} d \theta, \quad(11)
\end{aligned}$$

where  $G_\Lambda$ ,  $G_{\Lambda_{sd}}$ ,  $G_{\Lambda_{M_{u_i} d}^{u_i}}$  are the moment generating functions (MGF) of  $\Lambda$ ,  $\Lambda_{sd}$ , and  $\Lambda_{M_{u_i} d}^{u_i}$ , respectively. Equation (10) follows from Craig's formula [14]. We derive a closed-form expression of the integral in (11) as follows. Consider the following approximation of the integral in (11):

$$P(E|\psi = \mathbb{U}) \cong \frac{1}{\pi} \int_0^{\frac{\pi}{2}}\left(1+\frac{\Omega_{eq}}{2 \sin ^2 \theta}\right)^{-(n+1) n_d} d \theta, \quad(12)$$

where  $\Omega_{eq}=\left(\Omega_{sd} \prod_{i=1}^n \Omega_{M_{u_i} d, u_i}\right)^{\frac{1}{n+1}}$ . A closed-form expression of the integral in (12) is obtained from MATHEMATICA as

$$\begin{aligned}
&\frac{1}{\pi} \int_0^{\frac{\pi}{2}}\left(1+\frac{\Omega_{eq}}{2 \sin ^2 \theta}\right)^{-(n+1) n_d} d \theta \\
&=\frac{1}{\pi} \frac{1}{2\left(1+\frac{\Omega_{eq}}{2}\right)^{\frac{3}{2}}(n+1) \Gamma(n+1)}\left[\left(1+\frac{2}{\Omega_{eq}}\right)^{-n-\frac{1}{2}}\right. \\
&\frac{\Omega_{eq}}{2}^{-n-1} \sqrt{\pi}\left(\sqrt{\frac{\Omega_{eq}}{2}}\left(1+\frac{\Omega_{eq}}{2}\right)^{n+2}(n+1) \sqrt{\pi} \Gamma(n+1)+\right. \\
&\left.\left.\left(1+\frac{\Omega_{eq}}{2}\right)^{\frac{1}{2}} \Gamma\left(n+\frac{3}{2}\right)\left\{{}_2 F_1\left(1, n+\frac{3}{2},-\frac{1}{2}, \frac{\Omega_{eq}}{\Omega_{eq}+2}\right)\right.\right. \right. \\
&+\left.\left.\left.-1+\Omega_{eq}(n+2)\right)_2 F_1\left(1, n+\frac{3}{2}, \frac{1}{2}, \frac{\Omega_{eq}}{\Omega_{eq}+2}\right)\right)\right], \quad(13)
\end{aligned}$$

where  $\Gamma(\alpha)$  is the gamma function with argument  $\alpha$  and  ${}_2 F_1(\cdot, \cdot; \cdot; \cdot)$  is hypergeometric function. The numerical results in Section IV shows that the analytical BER obtained by using the closed-form expression in (13) closely follows the simulation results.

Now,  $P(\psi = \mathbb{U})$  can be written as

$$P(\psi = \mathbb{U}) = \prod_{l \in \mathbb{U}} P(A_l) \prod_{q \in \mathbb{U}^c} (1 - P(A_q)), \quad(14)$$

where  $A_l$  is the event that the index  $l$  of diversity branch  $B_l$  being in the set  $\mathbb{U}$ , the set  $\mathbb{U}^c \triangleq \{1, 2, \dots, L\} \setminus \mathbb{U}$ , and

$$P(A_l)=(1-P(E_{sr_1}^l)) \prod_{k=2}^{M_l}(1-P(E_{k-1,k}^l)). \quad(15)$$

$E_{sr_1}^l$  is the event of error in S-to- $R_{1,l}$  link,  $E_{M_l,d}^l$  is the event of error in  $R_{M_l,l}$ -to-D link, and  $E_{k-1,k}^l$  is the error event in  $R_{k-1,l}$ -to- $R_{k,l}$  link. From (2), the conditional probability of error  $P(E_{sr_1}^l | H_{sr_1,l})$  is given by  $Q(\sqrt{\Lambda_{sr_1,l}})$  [2], where  $\Lambda_{sr_1,l}=\frac{\| \mathbf{h}_{sr_1,l}^2-\mathbf{h}_{sr_1,l}^1 \|^2}{2 \sigma^2}$ .  $\mathbf{h}_{sr_1,l}^q$  is the  $q$ th column of  $\mathbf{H}_{sr_1,l}$ .

The average error probability  $P(E_{sr_1}^l)$  can be derived as

$$\begin{aligned}
&P(E_{sr_1}^l) \\
&=\int_0^{\infty} Q(\sqrt{\phi}) f_{\Lambda_{sr_1,l}}(\phi) d \phi \\
&=\int_0^{\infty} \int_{\sqrt{\phi}}^{\infty} \frac{e^{-\frac{v^2}{2}} d v}{\sqrt{2 \pi}} \frac{\phi^{n_{r_1,l}-1} \exp (-\frac{\phi}{\Omega_{sr_1,l}}) d \phi}{\Omega_{sr_1,l}^{n_{r_1,l}}(n_{r_1,l}-1)!} \\
&=\int_0^{\infty} \int_0^{v^2} \frac{\phi^{n_{r_1,l}-1} \exp (-\frac{\phi}{\Omega_{sr_1,l}}) d \phi}{\Omega_{sr_1,l}^{n_{r_1,l}}(n_{r_1,l}-1)!} \frac{e^{-\frac{v^2}{2}} d v}{\sqrt{2 \pi}} \quad(16)
\end{aligned}$$

$$=\int_0^{\infty}\left[1-\sum_{t=0}^{n_{r_1,l}-1}\left(\frac{v^2}{\Omega_{sr_1,l}}\right)^t \frac{\exp (-\frac{v^2}{\Omega_{sr_1,l}})}{t!}\right] \frac{e^{-\frac{v^2}{2}} d v}{\sqrt{2 \pi}} \quad(17)$$

$$=\frac{1}{2}\left[1-\sum_{t=0}^{n_{r_1,l}-1} \frac{\sqrt{\Psi_{sr_1,l}}}{\Omega_{sr_1,l}^t t!} \int_{-\infty}^{\infty} \frac{v^{2 t} \exp (-\frac{v^2}{2 \Psi_{sr_1,l}})}{\sqrt{2 \pi \Psi_{sr_1,l}}} d v\right] \quad(18)$$

$$=\frac{1}{2}\left[1-\sum_{t=0}^{n_{r_1,l}-1} \frac{\Psi_{sr_1,l}^{t+\frac{1}{2}}(2 t) !}{\Omega_{sr_1,l}^t 2^t t!}\right], \quad(19)$$

where  $\Psi_{sr_1,l}=\frac{\Omega_{sr_1,l}}{\Omega_{sr_1,l}+2}$ ,  $\Omega_{sr_1,l}=\frac{\sigma_{sr_1,l}^2}{\sigma^2}$ , (16) follows from change in the order of integral, and (17) follows from the definition of cumulative distribution of gamma random variable. Using the expression of the  $2t$ th central moment of normal r.v. (i.e.,  $\Psi_{sr_1,l}^t \frac{(2 t) !}{2^t t!}$ ) in (18), we get (19).  $P(E_{M_l,d}^l)$  and  $P(E_{k-1,k}^l)$  can be derived in a similar way, and is given by

$$P(E_{M_l,d}^l)=\frac{1}{2}\left[1-\sum_{t=0}^{n_d-1} \frac{\Psi_{M_l d, l}^{t+\frac{1}{2}}(2 t) !}{\Omega_{M_l d, l}^t 2^t t!}\right] \quad(20)$$

$$P(E_{k-1,k}^l)=\frac{1}{2}\left[1-\sum_{t=0}^{n_{k-1,k}^l-1} \frac{\Psi_{k-1,k,l}^{t+\frac{1}{2}}(2 t) !}{\Omega_{k-1,k,l}^t 2^t t!}\right], \quad(21)$$

where  $\Psi_{M_l d, l}=\frac{\Omega_{M_l d, l}}{\Omega_{M_l d, l}+2}$ ,  $\Psi_{k-1,k,l}=\frac{\Omega_{k-1,k,l}}{\Omega_{k-1,k,l}+2}$ ,  $\Omega_{k-1,k,l}=\frac{\sigma_{k-1,k,l}^2}{\sigma^2}$ .

### B. Approximate analysis for $n_s=2^m, m>1$

The end-to-end BER for the case of  $n_s=2$  derived in Section III-A is a function of the error probability of individual links, i.e.,  $P(E_{sr_1}^l)$ ,  $P(E_{k-1,k}^l)$ ,  $P(E_{M_l,d}^l)$ , as well as the conditional error probability at D for each realization of  $\psi$ , e.g.,  $P(E|\psi = \mathbb{U})$ . For  $n_s=2^m, m>1$ , i.e., non-binary SSK, we derive the approximate error probability using union bound approach. Our computation shows that if we directly apply the union bound on the end-to-end BER, then the resulting curve does not follow the simulated BER curve closely. Therefore, we have adopted a different approach whereby the union bound of each constituent probabilities of the end-to-end BER expression are obtained. The approximate BER expression is then derived using these union bound expressions in the similar manner as explained in Section III-A. The approximate BER thus obtained is not an upper bound on the

actual BER, since the actual BER is not a monotonically increasing function of every one of these constituent probabilities. The union bound of the probability terms are as follows

$$P(E_{sr_1}^l) \leq C_{eff} PEP(E_{s1}^l) = \tilde{P}(E_{sr_1}^l), \quad (22)$$

$$P(E_{k-1,k}^l) \leq C_{eff} PEP(E_{k-1,k}^l) = \tilde{P}(E_{k-1,k}^l), \quad (23)$$

$$P(E_{M_{ld}}^l) \leq C_{eff} PEP(E_{M_{ld}}^l) = \tilde{P}(E_{M_{ld}}^l), \quad (24)$$

$$P(E|\psi = \mathbb{U}) \leq C_{eff} PEP(E|\mathbb{U}) = \tilde{P}(E|\psi = \mathbb{U}), \quad (25)$$

where  $C_{eff} = \sum_{t=1}^{n_s} \sum_{p=1, p \neq t}^{n_s} \frac{N(\mathbf{s}_t \rightarrow \mathbf{s}_p)}{n_s \log_2(n_s)}$ , and  $N(\mathbf{s}_t \rightarrow \mathbf{s}_p)$  is the number of bits in error when  $\mathbf{s}_t$  is detected as  $\mathbf{s}_p$ .  $PEP(E_{s1}^l)$ ,  $PEP(E_{k-1,k}^l)$ ,  $PEP(E_{M_{ld}}^l)$ ,  $PEP(E|\mathbb{U})$  are the pairwise error probabilities, and are given by (19), (20), (21) and (13), respectively. Using the union bound expressions  $\tilde{P}(E_{sr_1}^l)$ ,  $\tilde{P}(E_{k-1,k}^l)$ ,  $\tilde{P}(E_{M_{ld}}^l)$ ,  $\tilde{P}(E|\psi = \mathbb{U})$  in place of  $P(E_{sr_1}^l)$ ,  $P(E_{k-1,k}^l)$ ,  $P(E_{M_{ld}}^l)$ ,  $P(E|\psi = \mathbb{U})$  in (6), (14), and (15), the closed-form expression of approximate BER is obtained.

#### IV. RESULTS AND DISCUSSION

We computed the BER as function of signal-to-noise-ratio (SNR) using the analytical expressions derived in the previous section. We also obtained the BER versus SNR curves through simulation for the purpose of comparison with the analytical BERs. We define SNR as  $\frac{1}{\sigma^2}$ . We keep the channel parameters as  $\sigma_{sr_1,l}^2 = \sigma_{k-1,k,l}^2 = \sigma_{M_{ld},l}^2 = \sigma_{sd}^2 = 0$  dB. Figure 2 presents the BER plots as a function of SNR for 3 branches ( $L = 2$  multi-hop branches and the direct S-to-D branch) with varying number of relays in each multi-hop branch ( $M_1 = M_2 = 2, 4$ ) obtained through simulation and analysis. The number of transmit and receive antennas is taken as 2 at all the nodes, i.e.,  $n_s = n_d = n_{r_k,l} = 2$ ;  $k = 1, \dots, 4$ ;  $l = 1, 2$ . The analytical and simulated BER plots show an almost exact match. Figure 3 shows the BER versus SNR plots for varying number of branches ( $L = 1, 2, 3$ ) with each multi-hop branch having 3 relays, obtained through analysis and simulation. The number of antennas is kept at 2 in all the nodes. Here also, the BER curves corresponding to analysis and simulation match almost exactly. These two figures validate the analysis presented in this paper for binary SSK.

Figure 4 shows the BER vs SNR plots for  $L = 2, 3$  relays in each multi-hop branch ( $M_1 = M_2 = 3$ ) for SSK with  $n_s = 2$  and  $n_s = 8$ . The number of receive antennas in each link for  $n_s = 2$  and  $n_s = 8$  are  $n_d = n_{r_i,l} = 2$ , and 8, respectively;  $i = 1, 2, 3$ ;  $l = 1, 2$ . It can be seen that, for  $n_s = 8$  also, the approximate analytical BER curve is close to the simulated BER curve. For the purpose of performance comparison with conventional PSK modulation, we have plotted the BER vs SNR plots for BPSK and 8-PSK with the same network setting with single transmit RF chain in each link. The number

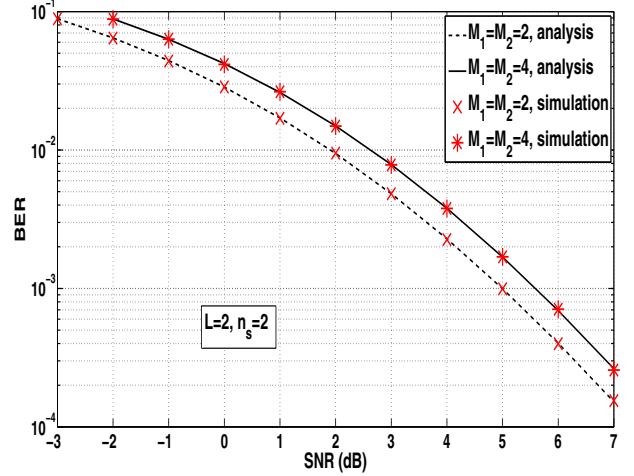


Fig. 2. BER versus SNR plots for SSK modulation in cooperative multi-hop multi-branch relaying, for  $L = 2$ , and 2, 4 relays in each diversity branch ( $M_1 = M_2 = 2, 4$ ).  $\sigma_{sr_1,l}^2 = \sigma_{k-1,k,l}^2 = \sigma_{M_{ld},l}^2 = \sigma_{sd}^2 = 0$  dB,  $l = 1, 2$ ;  $k = 2, 3, 4$ ,  $n_s = n_d = n_{r_i,l} = 2$ ;  $i = 1, 2, 3, 4$ ;  $l = 1, 2$ . Analysis and simulation.

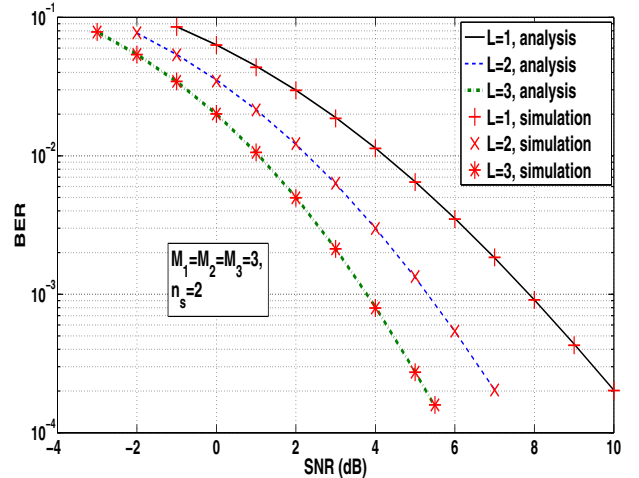


Fig. 3. BER versus SNR plots for SSK modulation in cooperative multi-hop multi-branch relaying, for  $L = 1, 2, 3$ , and 3 relays in each multi-hop branch ( $M_1 = M_2 = M_3 = 3$ ).  $\sigma_{sr_1,l}^2 = \sigma_{k-1,k,l}^2 = \sigma_{M_{ld},l}^2 = \sigma_{sd}^2 = 0$  dB,  $l = 1, 2$ ;  $k = 2, 3$ ,  $n_s = n_d = n_{r_i,l} = 2$ ;  $i = 1, 2, 3$ ;  $l = 1, 2, 3$ . Analysis and simulation.

of receive antennas in each link is taken to be 2 for BPSK, and 8 for 8-PSK ( $n_d = n_{r_i,l} = 2, 8$ ;  $i = 1, 2, 3$ ;  $l = 1, 2$ ). The figure shows that binary SSK is outperformed by BPSK, whereas SSK with  $n_s = 8$  shows significantly better BER performance than 8-PSK.

#### V. CONCLUSION

We derived closed-form expressions for the end-to-end BER for SSK modulation in cooperative multi-hop multi-branch relay networks. We considered DF relaying, where the relays forwarded the decoded signal only when they decode the signal correctly. For binary SSK, we derived a closed-form anal-

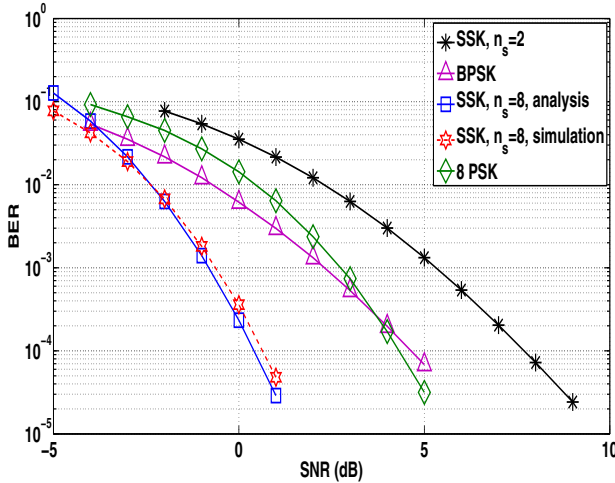


Fig. 4. BER versus SNR plots for SSK modulation ( $n_s = 2/8$ ) in cooperative multi-hop multi-branch relaying, for  $L = 2$  and 3 relays in each multi-hop branch ( $M_1 = M_2 = 3$ ).  $\sigma_{sr_{1,l}}^2 = \sigma_{1,2,l}^2 = \sigma_{2,3,l}^2 = \sigma_{3d,l}^2 = \sigma_{sd}^2 = 0$  dB,  $l = 1, 2$ ,  $n_d = n_{ri,l} = 2$  (for BPSK and SSK with  $n_s = 2$ ), 8 (for 8-PSK and SSK with  $n_s = 8$ );  $i = 1, 2, 3$ ;  $l = 1, 2$ . Single transmit RF chain for BPSK and 8-PSK in each link.

lytical expression for the BER. For SSK with more than two transmit antennas, the analytical BER is derived using union bound approximation. Numerical results showed that the analytical BER follows the simulated BER closely. The results also showed that SSK with eight transmit antennas outperforms 8-PSK in the considered network setting.

## REFERENCES

- [1] M. Di Renzo, H. Haas, and P. M. Grant, "Spatial modulation for multiple-antenna wireless systems: a survey," *IEEE Commun. Mag.*, vol. 50, no. 12, pp. 182-191, Dec. 2011.
- [2] J. Jeganathan, A. Ghrayeb, L. Szczerzinski, and A. Ceron, "Space shift keying modulation for MIMO channels," *IEEE Trans. Wireless Commun.*, vol. 8, no. 7, pp. 3692-3703, Jul. 2009.
- [3] N. Serafimovski, S. Sinanovic, M. Di Renzo, and H. Haas, "Dual-hop spatial modulation (Dh-SM)," *Proc. IEEE VTC'2011-Spring*, pp. 1-5, May 2011.
- [4] S. Sugiura, S. Chen, H. Haas, P. M. Grant, and L. Hanzo, "Coherent versus non-coherent decode-and-forward relaying aided cooperative space-time shift keying," *IEEE Trans. Commun.*, vol. 59, no. 6, pp. 1707-1719, Jun. 2011.
- [5] D. Yang, C. Xu, L.-L. Yang, and L. Hanzo, "Transmit-diversity-assisted space-shift keying for collocated and distributed/cooperative MIMO elements," *IEEE Trans. Veh. Tech.*, vol. 60, no. 6, pp. 2864-2869, Jul. 2011.
- [6] Y. Yang and S. Aissa, "Information-guided transmission in decode-and-forward relaying systems: spatial exploitation and throughput enhancement," *IEEE Trans. Wireless Commun.*, vol. 10, no. 7, pp. 2341-2351, Jul. 2011.
- [7] R. Mesleh, S. Ikki, and M. Alwakeel, "Performance analysis of space shift keying with amplify and forward relaying," *IEEE Commun. Lett.*, vol. 15, no. 12, pp. 1350-1352, Dec. 2011.
- [8] R. Mesleh, S. Ikki, H. M Aggoune, and A. Mansour, "Performance analysis of space shift keying (SSK) modulation with multiple cooperative relays," *Eurasip Jl. on Advances in Signal Processing*, doi:10.1186/1687-6180-2012-201, Sep. 2012.
- [9] A. Riberio, X. Cai, and G. Giannakis, "Symbol error probabilities for general cooperative links," *IEEE Trans. Wireless Commun.*, vol. 4, no. 3, pp. 1264-1273, May 2005.
- [10] G. Farhadi and N. C. Beaulieu, "On the performance of amplify-and-forward cooperative systems with fixed gain relays," *IEEE Trans. Wireless Commun.*, vol. 7, no. 5, pp. 1851-1856, May 2008.
- [11] M. D. Renzo, F. Graziosi, and F. Santucci, "A unified framework for performance analysis of CSI-assisted cooperative communications over fading channels," *IEEE Trans. Commun.*, vol. 57, no. 9, pp. 2551-2557, Sep. 2009.
- [12] M. D. Renzo, F. Graziosi, and F. Santucci, "A comprehensive framework for performance analysis of cooperative multi-hop wireless systems over log-normal fading channels," *IEEE Trans. Commun.*, vol. 58, no. 2, pp. 531-544, Feb. 2010.
- [13] A. H. Forghani, S. S. Ikki, and S. Aissa, "Performance evaluation of multi-hop multi-branch relaying networks with multiple co-channel interferers," *Proc. IEEE ICC 2012*, June 2012.
- [14] J. W. Craig, "A new, simple and exact result for calculating the probability of error for two-dimensional signal constellations," *Proc. IEEE MILCOM'91*, Nov. 1991.